



Pharmaceutical nanotechnology

Uniform nano-sized valsartan for dissolution and bioavailability enhancement: Influence of particle size and crystalline state

Qiuping Ma^a, Hongrui Sun^b, Erxi Che^a, Xin Zheng^a, Tongying Jiang^a, Changshan Sun^a, Siling Wang^{a,*}^a Department of Pharmaceutics, School of Pharmacy, Shenyang Pharmaceutical University, Wenhua Road 103, Shenyang 110016, PR China^b English Teaching Department, School of Basic Courses, Shenyang Pharmaceutical University, Wenhua Road 103, Shenyang 110016, PR China

ARTICLE INFO

Article history:

Received 17 September 2012

Received in revised form 6 November 2012

Accepted 15 December 2012

Available online xxx

Keywords:

Valsartan

Nanosuspension

Particle size

Crystalline state

Dissolution

Bioavailability

ABSTRACT

The central purpose of this study was to evaluate the impact of drug particle size and crystalline state on valsartan (VAL) formulations in order to improve its dissolution and bioavailability. VAL microsuspension (mean size 22 μm) and nanosuspension (30–80 nm) were prepared by high speed dispersing and anti-solvent precipitation method and converted into powders through spray drying. Differential scanning calorimetry studies indicated amorphization of VAL in the spray-dried valsartan nanosuspension (SD-VAL-Nano) but recrystallization occurred after 6 months storage at room temperature. The spray-dried valsartan microsuspension (SD-VAL-Micro) conserved the crystalline form. The VAL dissolution rate and extent were markedly enhanced with both SD-VAL-Micro and SD-VAL-Nano as compared to crude VAL crystals over the pH range of 1.2–6.8. Pharmacokinetic studies in rats demonstrated a 2.5-fold increase in oral bioavailability in the case of SD-VAL-Nano compared with the commercial product while the SD-VAL-Micro provided a much less desirable pharmacokinetic profile. In conclusion, reducing particle size to the nano-scale appears to be a worthwhile and promising approach to obtain VAL products with optimum bioavailability. In addition, the impact of crystalline state on the bioavailability of nano-sized VAL might be not as big as that of particle size.

© 2012 Elsevier B.V. All rights reserved.

1. Introduction

An essential physicochemical property of a drug is solubility, especially aqueous system solubility. For a drug to enter the systemic circulation and exert a therapeutic effect, it must first be in solution. Given that 40% or more of new chemical entities are poorly water soluble (classes II and IV in the biopharmaceutical system) and thereby suffer from low bioavailability or erratic absorption, formulations of these substances pose a significant challenge for the development of viable dosage forms during early stages of drug development.

Pharmaceutical nanosuspensions are colloidal dispersions of pure drug nanoparticles stabilized by suitable surfactants with the particle size of the nanoparticles being typically in the range 200–600 nm. Nanosuspension preparation can be broadly classified into two categories: bottom-up processes (precipitation-hydrosols, Nanomorph[®]) and top-down processes (bead milling-NanoCrystal[®], high pressure homogenization-DissoCubes[®],

NANOEDGE[®]) (Müller et al., 2011; Verma et al., 2009). Since their first introduction in the 1990s, nanosuspensions have become increasingly popular in pharmaceutical R&D to tackle poor bioavailability issues associated with poorly water-soluble drugs (Kayser et al., 2003). One of the benefits of nanosuspensions is their positive effect on oral absorption and bioavailability. Improved bioavailability can be attributed to enhanced bioadhesiveness of drug nanoparticles to the mucosa, increased saturation solubility leading to an increase concentration gradient between the gastrointestinal tract lumen and blood and the increased dissolution velocity of the drug (Rabinow, 2004). Other advantages of nanosuspensions include ease of manufacture and scale-up, general applicability to most drugs and versatility in surface modification (Patravale et al., 2004). Nanosuspensions are developing as the most successful nanotechnology, with a large number of products currently on the market and in clinical phases (Shegokar and Müller, 2010).

Valsartan (VAL) is an orally active specific antagonist of the angiotensin II AT₁-receptor that has been widely used in the treatment of mild to moderate hypertension. VAL is rapidly absorbed after oral administration but unfortunately suffers from inadequate and erratic bioavailability of about 23% mainly attributed to its low aqueous solubility at lower pH (Flesch et al., 1997). Number of formulation attempts have been made to address the low solubility and low bioavailability of VAL including solid dispersions (Yan

* Corresponding author at: Shenyang Pharmaceutical University, P.O. Box 32, 103 Wenhua Road, Shenhe District, Shenyang, Liaoning Province 110016, China. Tel.: +86 24 23986348; fax: +86 24 23986348.

E-mail address: silingwang@syphu.edu.cn (S. Wang).

et al., 2012), β -cyclodextrin complexes (Cappello et al., 2006), microcapsules (Li et al., 2010), and use of recrystallization technique (Youn et al., 2011). However, the *in vivo* effect of the particle size and crystalline state of VAL have not been examined in detail till date according to current literature review. In the present study, VAL nanosuspension and its spray-dried powders were successfully formulated for dissolution and bioavailability enhancement of the drug. To allow a comparison, microsuspension of VAL was also prepared. We focused on evaluating the influence of particle size and crystalline state on the *in vitro* and *in vivo* performance of VAL.

2. Materials and methods

2.1. Materials

Valsartan was supplied as micronized powder from Changzhou Kony Pharm Co., Ltd. (Chang zhou, Jiangsu, China). Poloxamer 407 (Lutrol® F-127) and AEROSIL®200 were obtained as gift samples from BASF (Ludwigshafen, Germany) and Degussa (Darmstadt, Germany), respectively. HPLC grade acetonitrile and methanol were purchased from Concord Chemical Agent Company (China). Double-distilled deionized water was used in all experiments and all other chemicals used were of analytical grade.

2.2. Preparation of VAL microsuspension and nanosuspension

The VAL microsuspension was obtained by suspending 1 g of crude drug powders, preferably micronized particles, in 300 ml of aqueous surfactant solution containing 0.2% poloxamer 407 and stirring with Ultra-Turrax T10 Basic (IKA, Germany) at 8000 rpm for approximately 5 min. The VAL nanosuspension was prepared by a bottom-up precipitation method. In brief, 10 ml of VAL solution in methanol (100 mg/ml) was injected into 300 ml of poloxamer 407 (0.2%, w/v) solution under magnetic stirring at 800 rpm. To evaluate the possible effect of temperature and stirring rate on the particle diameters, formulations were prepared at different temperatures but with the same stirring rate (800 rpm) and characterized by particle size measurements.

The VAL nanosuspension could also be made by a top-down high pressure homogenization method. VAL nanosuspension was produced by subjecting the microsuspension obtained to an AH100D high pressure homogenizer (ATS Engineering Inc., Shanghai, China), operated at 200 bar for 5 cycles and 400 bar 5 cycles and 600 bar 10 cycles. The homogenizing chamber was cooled by circulating ethanol at 5 °C.

2.3. Spray drying

Spray-drying was performed to convert suspensions into dry powders, which were more stable, easily handled and stored and cost-effective than its liquid counterparts. Prior to the drying process, 200% AEROSIL®200 (relative to VAL weight, w/w) was added to the suspensions as a matrix former in order to inhibit nanoparticles agglomeration and preserve the original particle size. AEROSIL®200 was also used as an adsorbent to avoid the problem of stickiness (possibly due to hygroscopicity and amorphism of the dried powders and relatively lower glass transition temperature of VAL) (Ambike et al., 2005; Downton et al., 1982; Skotnicki et al., 2012) encountered in our previous formulations without. Spray drying was then operated with a laboratory scale EYELA SD-1000 spray drier (Tokyo Rikakikai Co., Ltd., Japan) under the following conditions: inlet air temperature, 110 °C; outlet air temperature, 60–65 °C; drying air flow rate, 0.5 m³/min; feed rate, 4 ml/min; atomization pressure, 170 kPa. During the process, the suspension was continuously stirred with a magnetic

stirrer. The resulting spray-dried valsartan micro- and nanosuspension powders (abbreviated to 'SD-VAL-Micro' and 'SD-VAL-Nano', respectively) contained micro- and nano-sized VAL, respectively. The powders were collected, vacuum dried at room temperature overnight and stored in a desiccator until physicochemical and pharmaceutical analysis.

2.4. Particle size measurement

The intensity-averaged particle sizes of the VAL nanosuspensions were measured by dynamic light scattering (Malvern Zetasizer) at 25 °C. Particle size in the range of 3 nm to 10 μ m can be determined by this instrument. The volume-averaged particle size of the VAL microsuspension was measured by laser diffraction (Coulter LS 230) at 25 °C. All measurements were made in triplicate.

2.5. Physical stability of VAL nanosuspension

To preliminarily investigate the short-term stability of the nanosuspensions, nanosuspensions were kept at closed glass vial and stored at 25 °C. During 7 days of monitoring, particle size and PDI were determined. Day 0 was the day of production.

2.6. Differential scanning calorimetry (DSC)

The crystalline properties of the formulated samples were assessed by differential scanning calorimetry according to the procedure described by Hu et al. (2011) with a DSC 1 STAR[®] instrument (Mettler Toledo, Switzerland).

2.7. In vitro dissolution

Dissolution testing was conducted utilizing an USP II dissolution apparatus (Tianjin University Electronics Co., Model ZRS-8G). An amount of powders equivalent to 80 mg of VAL were dispersed in 1000 ml various media (0.1 M HCl, pH 1.2; acetate buffer solution, pH 4.0; phosphate buffer solution, pH 6.8; and distilled water) maintain at 37 \pm 0.5 °C and at a rotation speed of 100 rpm. At pre-determined time intervals, aliquots of 5 ml were withdrawn from the dissolution vessel, filtered through a 0.22 μ m membrane, and analyzed by a UV spectrophotometer at 250 nm. The dissolution experiment was done in triplicates for each sample, and the mean cumulative release was plotted.

2.8. In vivo studies

2.8.1. Animal experiments

The Male Sprague-Dawley rats (220 \pm 20 g) were randomly divided into four groups of 6 each. All rats were fasted overnight prior to dosing but allowed free access to water. The four groups were orally administrated the SD-VAL-Micro powders, the SD-VAL-Nano powders, the SD-VAL-Nano powders after 6 months storage (SD-VAL-Nano-6 months), and the commercial product Diovan[®] (as reference) at a dose of 10 mg/kg, respectively. At specified time intervals retro-orbital blood samples were collected into 0.5 ml heparinized centrifuge tubes. The tubes were immediately centrifuged for 10 min at 5000 \times g to collect the plasma, which was transferred to a new tube and stored frozen at –20 °C until analysis. All experiments were carried out in accordance with the NIH Guidelines for the Care and Use of Laboratory Animals and were approved by the Animal Ethics Committee, Shenyang Pharmaceutical University.

2.8.2. Plasma sample preparation and analysis

Blood samples were processed using acetonitrile protein precipitation method. Briefly, to a blood sample (100 μ l), 7.5 μ l of internal

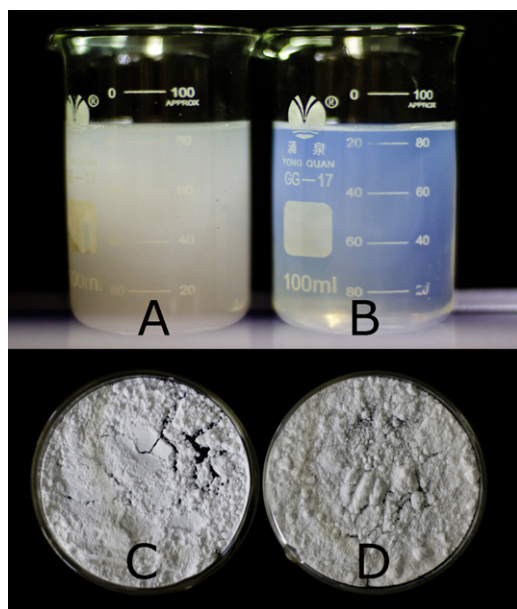


Fig. 1. Visual comparison of the VAL micro-suspension (A), nanosuspension (B) (prepared at 25 °C and 800 rpm) and their spray-dried powders, SD-VAL-Micro (C) and SD-VAL-Nano (D), respectively.

standard solution (telmisartan, 4 µg/ml) was spiked and 1 ml of acetonitrile added. The mixture was vortex-mixed for 1 min and subsequently centrifuged 5 min at 5000 × g. 10 µl supernatant was injected into HPLC for quantification of VAL.

The HPLC analysis system consisted of L-2130 pump, L-2485 fluorescence detector, L-2300 column oven and L-2200 auto sampler. An Ecosil C18 column (250 mm × 4.6 mm, i.d., 5 µm), protected by a guard column (10 mm × 4.6 mm, i.d.) was used at 40 °C, with a mobile phase composed of potassium dihydrogen phosphate (10 mM; pH 3.0)–methanol–acetonitrile (32:44:24, v/v/v) at 1.5 ml/min. The eluent was monitored at 265 nm/378 nm (excitation/emission wavelength).

2.8.3. Pharmacokinetic data analysis

The area under the plasma concentration time curve (AUC_{0-t}) was calculated using a two-compartmental model through drug and statistics software (DAS® 2.1, Boying Corporation, China). The maximum plasma peak concentration of the drug (C_{max}) and the time to reach the peak concentration (T_{max}) were obtained directly from the plasma data. The relative bioavailability values (F) were calculated according to the following formula with the commercial product Diovan® as reference:

$$F(\%) = \frac{AUC_{test}}{AUC_{reference}} \times 100$$

All data were expressed as the mean ± standard deviation (S.D.). The statistical analysis was made using the *t*-test. A *P* value less than 0.05 was considered statistically significant.

3. Results

3.1. Appearance

As could be clearly seen from Fig. 1, the prepared VAL nanosuspension exhibited tense bluish opalescence, indicating successful formation of the nanodispersion of VAL. The VAL nanosuspension was transparent whereas the micro-suspension was turbid. Both the SD-VAL-Micro and SD-VAL-Nano were fine white powders with good flowability.

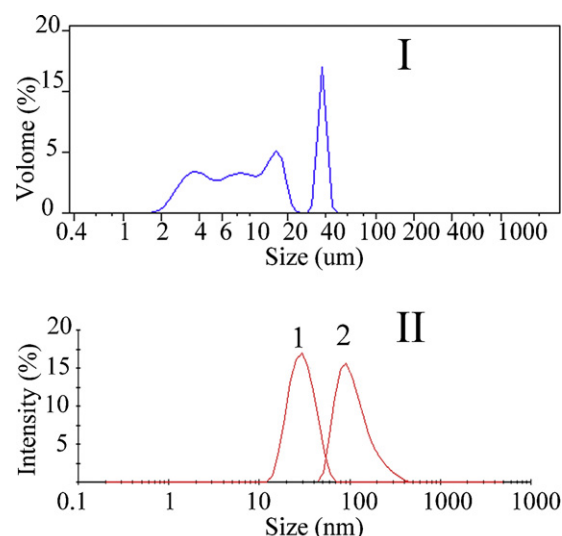


Fig. 2. Representative particle size distribution of the VAL micro-suspension (I) and nanosuspension (II). (1) Obtained by anti-solvent precipitation and (2) by high pressure homogenization.

3.2. Particle sizes of the VAL micro- and nanosuspension

Fig. 2 shows representative particle size distribution of the prepared suspensions. A rather broad distribution ranging from 2 µm to 60 µm was observed for the VAL micro-suspension. The VAL nanosuspension prepared by anti-solvent precipitation (25 °C, 800 rpm) clearly exhibited a tight and monodisperse intensity-based size distribution, with an average diameter of 30.7 nm and a polydispersity index value (PDI) of 0.086, suggesting the uniformity of the suspension. High pressure homogenization (HPH) resulted in VAL nanosuspension with a larger particle size (117 nm). During a 7-day period, particle size of the nanosuspension (obtained by precipitation) hardly increased. Uniformity of the dispersion might be a contributing factor to its remarkable physical stability that avoided Ostwald ripening.

Eventually, because of its simplicity, energy-efficiency and the smaller nanoparticles obtained, the anti-solvent precipitation technique was chosen as the optimal method of preparation and the obtained products were subjected to further processing.

3.3. Process parameter – temperature

From Fig. 3 and Table 1, it could be seen that temperature of production during the anti-solvent precipitation process affected the sizes of VAL nanosuspensions. Within the temperature of 10–25 °C, uniform particles with the smallest diameters (30–80 nm) were obtained and this range was the optimum temperature range for

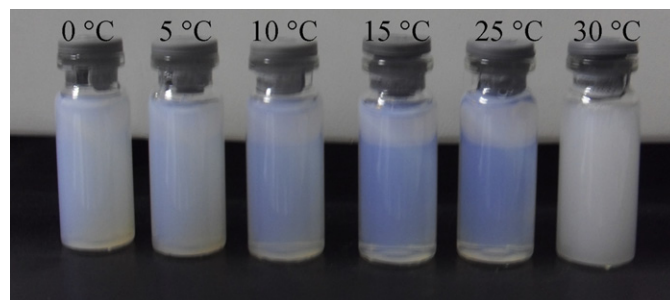


Fig. 3. Effect of production temperature on the particle size of VAL nanosuspension (by anti-solvent precipitation method).

Table 1

Average particle diameters and polydispersity index (PDI) of several formulations produced at different temperatures as a function of 7 days storage time (at 25 °C).

Day	Temperature (°C)											
	0		5		10		15		25		30	
	Size (nm)	PDI	Size (nm)	PDI	Size (nm)	PDI	Size (nm)	PDI	Size (nm)	PDI	Size (nm)	PDI
0	159.3	0.255	113.4	0.213	78.4	0.204	42.1	0.151	30.7	0.086	256.8	0.298
3	–	–	–	–	76.0	0.221	43.2	0.164	30.4	0.084	–	–
7	–	–	–	–	80.0	0.226	44.5	0.185	31.4	0.098	–	–

–, not determined.

preparing VAL nanosuspension. Outside this range, particle sizes increased considerably to about 260 nm at 30 °C and 160 nm at 0 °C but those diameters were still in the sub-micron range.

3.4. Short-term stability of the VAL nanosuspension

Hardly any changes were observed in particle size and PDI during 7 days of storage (25 °C) and this indicated that these nanosuspensions showed long-term stability promise.

3.5. DSC and XRD characterization

The DSC curve (Fig. 4) of crude VAL exhibited sharp endothermic peaks at 101.4 °C. In case of freshly made SD-VAL-Nano powders, no endothermic peak corresponding to VAL was observed, suggesting that the crystallinity of VAL dramatically decreased or the drug was possibly transformed into the amorphous state. It might as well be assumed that VAL in freshly made SD-VAL-Nano was amorphous, although with some arbitrariness. However, it was sure that the SD-VAL-Nano were in high energy state, whether they were in decreased crystalline state or amorphous state. The DSC pattern of the powders was monitored periodically to examine their potential transformation into low energy crystalline state over time. As expected, the melting peak of VAL was observed in SD-VAL-Nano samples after 6 months storage at ambient temperature, indicating that drug recrystallization had occurred. The melting peak of poloxamer 407 (around 45 °C) in SD-VAL-Micro and SD-VAL-Nano shifted towards a lower temperature with a concomitant broadening compared to pure poloxamer 407 (melting point 56.8 °C) could be ascribed to its decreased crystallinity and/or its interaction with

VAL and AEROSIL®200. The presence of VAL as an impurity might also have caused the melting point depression of poloxamer 407.

X-ray diffraction analysis (XRD) revealed all the characteristic diffraction peaks of VAL overlapped with those of poloxamer 407 (data not shown). Therefore, the presence of stabilizer poloxamer 407 interfered with the determination of the crystalline form of VAL in spray-dried powders in XRD analysis and XRD could not be used to determine the crystalline state of VAL. A previous study reported similar results (Park et al., 2010).

3.6. Dissolution tests

As illustrated in Fig. 5, the dissolution profiles of crude VAL displayed pronounced pH-dependence due to its weak acidity and its dissolution rate was very low at lower pH values. Only less than 10% of VAL dissolved within 60 min in pH 1.2 solution. A dramatic increase in both the dissolution rate and extent was observed with SD-VAL-Nano, as more than 80% of the drug dissolved within 10 min at various pHs. The SD-VAL-Micro also exhibited excellent dissolution behavior. During the first 10 min, drug dissolution was slightly lower than SD-VAL-Nano, but the cumulative percentage release of VAL reached approximately the same level as that of SD-VAL-Nano in 30 min. After 6 months storage, the dissolution of SD-VAL-Nano slightly decreased, possibly because of drug recrystallization and/or potential particle size growth and agglomeration.

The marked dissolution enhancement observed with micro-sized spray-dried VAL powders could be contributed to the increased surface area although the same effect was more pronounced for nano-sized VAL (Keck and Müller, 2006). We assumed that the increase *in vitro* dissolution rate might favourably affect the bioavailability.

3.7. Bioavailability study

The plasma concentrations and pharmacokinetic parameters of VAL after oral administration of the commercial product, SD-VAL-Micro and SD-VAL-Nano before and after 6 months storage at ambient conditions were shown in Fig. 6 and Table 2. The plasma concentration after administration of the freshly made SD-VAL-Nano was significantly higher than that of the commercial product. The C_{max} increased 1.8-fold and the AUC_{0-t} 2.5-fold. SD-VAL-Micro exhibited a similar plasma profile to the commercial product and no significant differences in pharmacokinetic parameters were observed between the two groups. The comparison between nano- and micro-sized VAL had clearly proven the advantages of using VAL nanosuspensions to achieve enhanced bioavailability. Although the SD-VAL-Nano underwent recrystallization at the end of the 6 months storage period, its *in vivo* performance was not significantly compromised, as F was slightly reduced from 251.48% to 230.84% and no statistically significant differences ($P > 0.05$) were found in C_{max} , T_{max} and AUC_{0-t} between the SD-VAL-Nano and SD-VAL-Nano-6 months powders. However, it was worth noting that the large error bars of SD-VAL-Nano in the plasma concentration-time curve suggested that nano-sized VAL

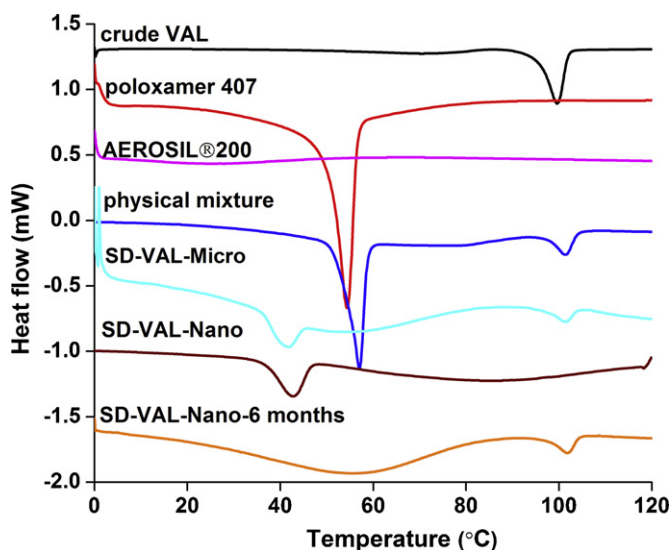


Fig. 4. DSC thermograms of the crude VAL, blank excipients, physical mixtures and spray-dried powders.

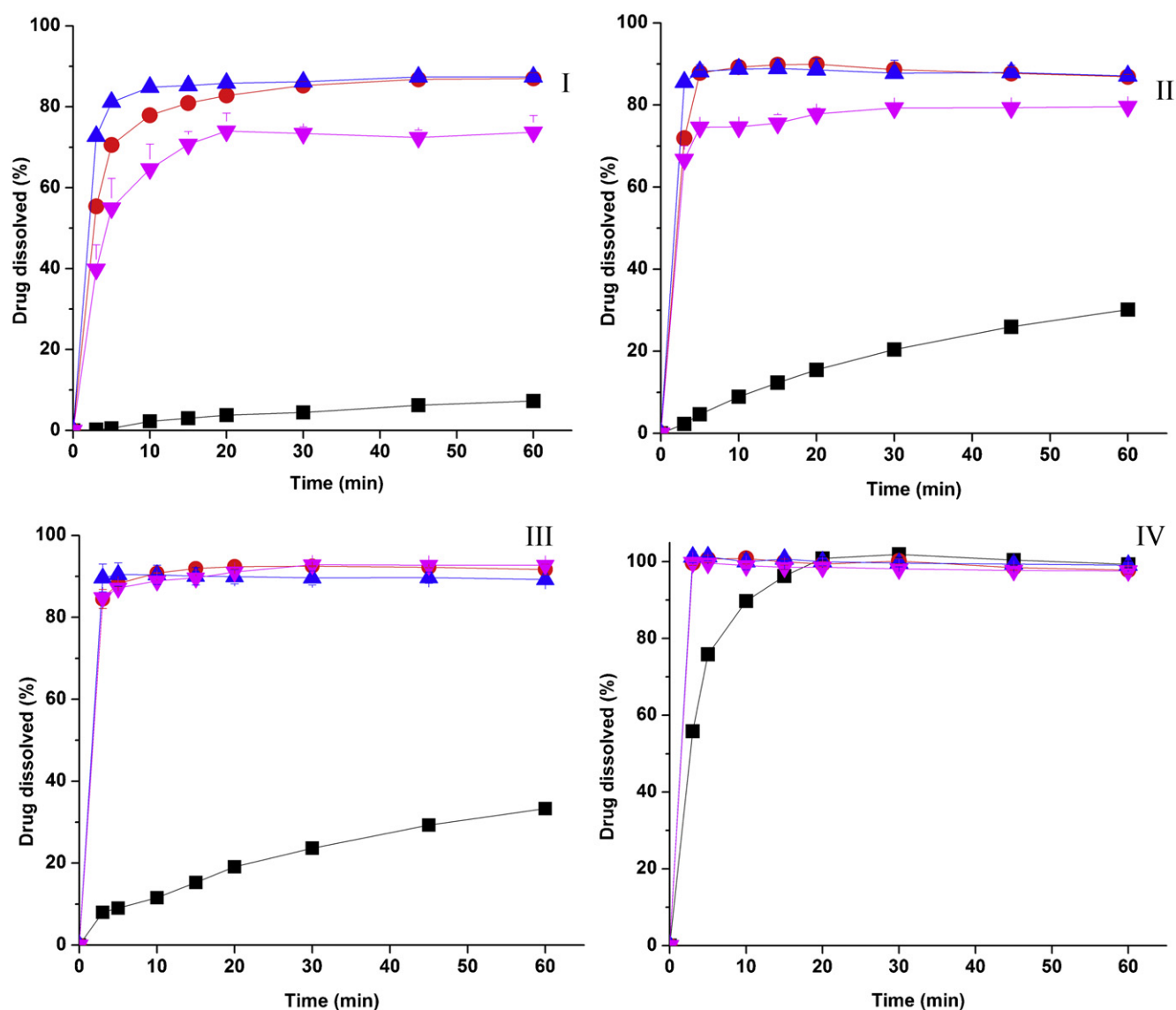


Fig. 5. Dissolution profiles of crude VAL (■), SD-VAL-Micro (●), SD-VAL-Nano before (▲) and after 6 months storage (▼) at pH 1.2 (I), at pH 4.0 (II), in distilled water (III) and at pH 6.8 (IV).

failed to address the erratic bioavailability issue of VAL. This might be due to the presence of VAL nanoparticles aggregates (discussed in Section 4.2).

4. Discussion

4.1. Particle size of the VAL nanosuspension

Uniform valsartan nanosuspension with an average diameter 30–80 nm was successfully prepared using a facile anti-solvent

precipitation method over a wide temperature range of 10–25 °C. The suspension showed long-term stability promise, as the particle size and PDI hardly changed after 7 days storage at 25 °C. Such small particle size of the nanosuspension fell into the category of smart crystals (<100 nm), the second generation of drug nanocrystals possessing improved physicochemical properties (Keck et al., 2008). Smart crystals immediately dissolve after i.v. injection and mimic solution pharmacokinetics (Müller and Keck, 2012). Hopefully, this nanoformulation might be applicable to intravenous administration.

Table 2

Pharmacokinetic parameters of VAL following oral administration (mean ± S.D., *n* = 6).

Parameters	The commercial product	SD-VAL-Micro	SD-VAL-Nano	SD-VAL-Nano-6 months
C_{max} (μg/ml)	11.07 ± 5.48	8.99 ± 4.40	20.41 ± 6.90*	20.63 ± 6.48*♦
T_{max} (h)	0.92 ± 0.38	1.25 ± 0.42	0.79 ± 0.19	0.75 ± 0.39♦
AUC_{0-t} (μg h/ml)	40.27 ± 22.72	45.08 ± 23.78	101.27 ± 29.46*	92.96 ± 14.15*♦
<i>F</i>	100%	111.94%	251.48%	230.84%

**P* < 0.05 compared to the commercial product.

♦*P* > 0.05 compared to SD-VAL-Nano.

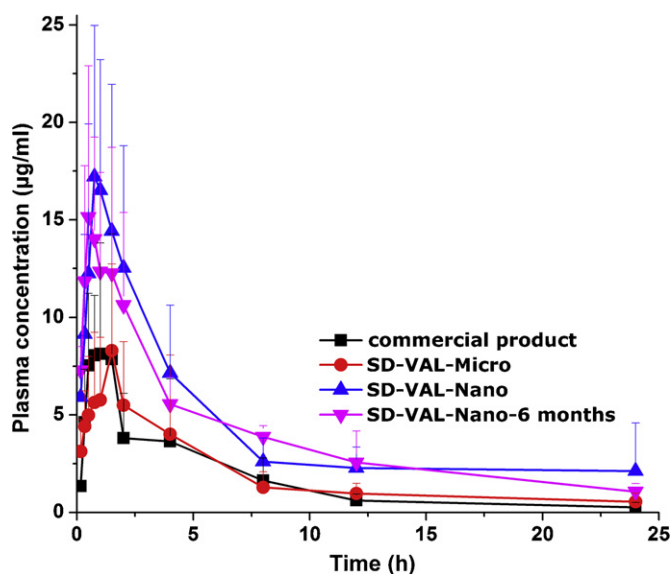


Fig. 6. Average plasma concentration–time profiles of VAL following oral administration at a dose of 10 mg/kg in rats (mean \pm S.D., $n = 6$).

4.2. Particle size growth and agglomeration

Prior to spray drying, different matrix formers were added to suspensions in order to inhibit nanoparticles agglomeration and preserve the original particle size. AEROSIL®200 was found to be the optimal because the spray-dried powders obtained showed faster and more complete dissolution profiles compared with what used other matrix formers, such as mannitol, sucrose, spray-dried lactose, trehalose and PVP K30 (data not shown). AEROSIL®200 is an insoluble silica material with a mean primary particle size of 12 nm (data of company). Aqueous suspensions of AEROSIL®200 show tri- or bimodal particle size distributions between 20 nm and 50 μ m (Gun'ko et al., 2001). Therefore, the particle size of VAL in SD-VAL-Nano after redispersing in water could not be directly measured because of the interference of AEROSIL®200. Hence potential particle size growth and agglomeration after spray drying could not be directly determined. Similar systems using AEROSIL®200 and other insoluble matrix former did not investigate the particle size changes of drugs after the spray drying and freeze drying processes (Van Eerdenbrugh et al., 2008a,b).

The slight decrease in dissolution rate of SD-VAL-Nano after 6 months storage in dissolution tests particle size growth and agglomeration might have occurred during storage period. The erratic bioavailability of SD-VAL-Nano and SD-VAL-Nano-6 months also indicated particles agglomeration because variability in disintegration and dissolution times due to the presence of aggregates could cause unpredictable variations in bioavailability (Chaubal and Popescu, 2008). However, the particle growth and agglomeration did not significantly affect the *in vitro* and *in vivo* performance of VAL.

4.3. Crystalline state

From a theoretical point of view, ideal drug nanosuspensions should be amorphous because amorphous drugs possess maximum solubility advantage in comparison with the crystalline form of the drug and thus better bioavailability (Keck et al., 2008). However, high energy amorphous materials are thermodynamically unstable and prone to revert to the crystalline form over time (Hancock and Zografi, 1997) and this may lead to decreased dissolution and thereby bioavailability (Singhal and Curatolo, 2004). Therefore, preservation of the amorphous state over the shelf-life of

pharmaceutical products is generally a problem. Similarly, in this study recrystallization of VAL was observed in SD-VAL-Nano at the end of the 6 months storage but the *in vitro* and *in vivo* performances were not significantly compromised. We assumed that perhaps the effect of crystalline state on the bioavailability of VAL nanoformulations was not big as that of particle size. It was necessary to conduct further studies to reach a persuasive conclusion.

4.4. Possible mechanism of enhanced absorption of nano-sized VAL

Although markedly enhanced dissolution *in vitro* was observed for the spray-dried microsuspension powders, their *in vivo* performance was adversely affected. This result suggested that reductions in VAL particle sizes increased drug uptake not only by dissolution but also by other routes. There was evidence that when particle size was reduced to the nanometer level, the uptake of intact gastrointestinal polymeric particles occurred (Florence and Hussain, 2001; Jani et al., 1990), by mechanisms involving M-cells in Peyer's patches of the gastrointestinal lymphoid tissue (Clark et al., 2001). Intact uptake of mesoporous silica nanoparticles (30–90 nm) was also observed and cellular uptake increased with decreasing particle diameter (Zhang et al., 2012). It was anticipated that intact uptake of the nano-sized VAL might be occurred, which was responsible for enhanced bioavailability of VAL. Additional studies are necessary to confirm this hypothesis.

5. Conclusion

In conclusion, we have demonstrated the superior *in vivo* performance of spray dried nano-sized VAL compared with micro-sized VAL and the commercial product. The particle size appears to play a significant role in the oral bioavailability of VAL. These results suggest that nanosuspension combined with spray drying is a worthwhile and promising strategy for increasing dissolution rate and oral bioavailability of VAL. Careful attention should be paid to the particle size growth, considering the potential physical stability of spray-dried VAL nanoproducts during storage. The impact of crystalline state on the bioavailability of nano-sized VAL might not be as big as that of particle size. Certainly, more research is needed to obtain further information about VAL nanoformulations and their stability issues.

Acknowledgements

This work was supported by the National Basic Research Program of China (973 Program) (No. 2009CB930300) and Major National Platform for Innovative Pharmaceuticals (2009ZX09301-012).

References

- Ambike, A.A., Mahadik, K.R., Paradkar, A., 2005. Spray-dried amorphous solid dispersions of simvastatin, a low tg drug: *in vitro* and *in vivo* evaluations. *Pharm. Res.* 22, 990–998.
- Cappello, B., Di Maio, C., Iervolino, M., Miro, A., 2006. Improvement of solubility and stability of Valsartan by hydroxypropyl-beta-cyclodextrin. *J. Incl. Phenom. Macro.* 54, 289–294.
- Chaubal, M.V., Popescu, C., 2008. Conversion of nanosuspensions into dry powders by spray drying: a case study. *Pharm. Res.* 25, 2302–2308.
- Clark, M., Jepson, M.A., Hirst, B.H., 2001. Exploiting M cells for drug and vaccine delivery. *Adv. Drug Deliv. Rev.* 50, 81–106.
- Downton, G.E., Flores-Luna, J.L., Kling, C.J., 1982. Mechanism of stickiness in hygroscopic, amorphous powders. *Ind. Eng. Chem. Fundam.* 21, 447–451.
- Flesch, G., Müller, P., Lloyd, P., 1997. Absolute bioavailability and pharmacokinetics of valsartan, an angiotensin II receptor antagonist, in man. *Eur. J. Clin. Pharmacol.* 52, 115–120.
- Florence, A.T., Hussain, N., 2001. Transcytosis of nanoparticle and dendrimer delivery systems: evolving vistas. *Adv. Drug. Deliv. Rev.* 50, S69–S89.

- Gun'ko, V.M., Zarko, V.I., Leboda, R., Chibowski, E., 2001. Aqueous suspension of fumed oxides: particle size distribution and zeta potential. *Adv. Colloid Interface Sci.* 91, 1–112.
- Hancock, B.C., Zografi, G., 1997. Characteristics and significance of the amorphous state in pharmaceutical systems. *J. Pharm. Sci.* 86, 1–12.
- Hu, Y., Zhi, Z., Wang, T., Jiang, T., Wang, S., 2011. Incorporation of indomethacin nanoparticles into 3-D ordered macroporous silica for enhanced dissolution and reduced gastric irritancy. *Eur. J. Pharm. Biopharm.* 79, 544–551.
- Jani, P., Halbert, G.W., Langridge, J., Florence, A.T., 1990. Nanoparticle uptake by the rat gastrointestinal mucosa: quantitation and particle size dependency. *J. Pharm. Pharmacol.* 42, 821–826.
- Kayser, O., Olbrich, C., Yardley, V., Kiderlen, A.F., Croft, S.L., 2003. Formulation of amphotericin B as nanosuspension for oral administration. *Int. J. Pharm.* 254, 73–75.
- Keck, C., Kobierski, S., Mauludin, R., Müller, R.H., 2008. Second generation of drug nanocrystals for delivery of poorly soluble drugs: smart crystals technology. *Dosis* 24, 124–128.
- Keck, C.M., Müller, R.H., 2006. Drug nanocrystals of poorly soluble drugs produced by high pressure homogenisation. *Eur. J. Pharm. Biopharm.* 62, 3–16.
- Li, D.X., Yan, Y.D., Oh, D.H., Yang, K.Y., Seo, Y.G., Kim, J.O., Kim, Y.I., Yong, C.S., Choi, H.G., 2010. Development of valsartan-loaded gelatin microcapsule without crystal change using hydroxypropylmethylcellulose as a stabilizer. *Drug Deliv.* 17, 322–329.
- Müller, R.H., Shegokar, R., Gohla, S., Keck, C.M., 2011. Nanocrystals: production, cellular drug delivery, current and future products. *Intracell. Deliv.* 5, 411–432.
- Müller, R.H., Keck, C.M., 2012. Twenty years of drug nanocrystals: where are we, and where do we go? *Eur. J. Pharm. Biopharm.* 80, 1–3.
- Park, Y.J., Lee, H.K., Im, Y.B., Lee, W., Han, H.K., 2010. Improved pH-independent dissolution and oral absorption of valsartan via the preparation of solid dispersion. *Arch. Pharm. Res.* 33, 1235–1240.
- Patravale, V.B., Date, A.A., Kulkarni, R.M., 2004. Nanosuspensions: a promising drug delivery strategy. *J. Pharm. Pharmacol.* 56, 827–840.
- Rabinow, B.E., 2004. Nanosuspensions in drug delivery. *Nat. Rev. Drug Discov.* 3, 785–796.
- Shegokar, R., Müller, R.H., 2010. Nanocrystals: industrially feasible multifunctional formulation technology for poorly soluble actives. *Int. J. Pharm.* 399, 129–139.
- Singhal, D., Curatolo, W., 2004. Drug polymorphism and dosage form design: a practical perspective. *Adv. Drug Deliv. Rev.* 56, 335–347.
- Skotnicki, M., Gawel, A., Cebe, P., Pyda, M., 2012. Thermal behavior and phase identification of valsartan by standard and temperature-modulated differential scanning calorimetry. *Drug Dev. Ind. Pharm.* [Epub ahead of print].
- Van Erdenbrugh, B., Vercruysse, S., Martens, J.A., Vermant, J., Froyen, L., Van Humbeeck, J., Van den Mooter, G., Augustijns, P., 2008a. Microcrystalline cellulose, a useful alternative for sucrose as a matrix former during freeze-drying of drug nanosuspensions – a case study with itraconazole. *Eur. J. Pharm. Biopharm.* 70, 590–596.
- Van Erdenbrugh, B., Froyen, L., Van Humbeeck, J., Martens, J.A., Augustijns, P., Van Den Mooter, G., 2008b. Alternative matrix formers for nanosuspension solidification: dissolution performance and X-ray microanalysis as an evaluation tool for powder dispersion. *Eur. J. Pharm. Sci.* 35, 344–353.
- Verma, S., Gokhale, R., Burgess, D.J., 2009. A comparative study of top-down and bottom-up approaches for the preparation of micro/nanosuspensions. *Int. J. Pharm.* 380, 216–222.
- Yan, Y.D., Sung, J.H., Kim, K.K., Kim, D.W., Kim, J.O., Lee, B.J., Yong, C.S., Choi, H.G., 2012. Novel valsartan-loaded solid dispersion with enhanced bioavailability and no crystalline changes. *Int. J. Pharm.* 422, 202–210.
- Youn, Y.S., Oh, J.H., Ahn, K.H., Kim, M., Kim, J., Lee, Y.W., 2011. Dissolution rate improvement of valsartan by low temperature recrystallization in compressed CO₂: prevention of excessive agglomeration. *J. Supercrit. Fluids* 59, 117–123.
- Zhang, Y., Wang, J., Bai, X., Jiang, T., Zhang, Q., Wang, S., 2012. Mesoporous silica nanoparticles for increasing the oral bioavailability and permeation of poorly water soluble drugs. *Mol. Pharm.* 9, 505–513.